

Backstepping Control of Muscle Driven Systems with Redundancy Resolution

Humberto De las Casas* Hanz Richter*

* *Mechanical Engineering Department, Cleveland State University, Cleveland, OH 44115 USA.*

Abstract: Due to the several applications on Human-machine interaction (HMI), this area of research has become one of the most popular in recent years. This is the case for instance of advanced training machines, robots for rehabilitation, robotic surgeries and prosthesis. In order to ensure desirable performances, simulations are recommended before real-time experiments. These simulations have not been a problem in HMI on the side of the machine. However, the lack of controllers for human dynamic models suggests the existence of a gap for performing simulations for the human side. This paper offers to fulfill the previous gap by introducing a novel method based on a feedback controller for the dynamics of muscle-driven systems. The approach has been developed for trajectory tracking of systems with redundancy muscle resolution. To illustrate the validation of the method, a shoulder model actuated by a group of eight linkages, eight muscles and three degrees of freedom was used. The controller objective is to move the arm from a static position to another one through muscular activation. The results on this paper show the achievement of the arm movement, musculoskeletal dynamics and muscle activations.

1. INTRODUCTION

Research in human-machine interaction (HMI) has received a lot of attention in recent years. The reason that seems to indicate this fact is the several applications with potential opportunities in the areas of development. For instance, human training has shown enhancement through the use of robotic training machines capable of providing variable resistance based on the user requirements (De las Casas et al., 2017) (De las Casas et al., 2019). Furthermore, rehabilitation processes have been proved to be very efficient with the use of machines designed to help people with disabilities to recover their motor skills (Chang and Kim, 2013) (Schmidt et al., 2007). Besides, several improvements in the quality of walking have been reported for people with amputees by using prosthesis with energy regeneration (Khalaf et al., 2018) (Khalaf et al., 2015). And, in the same way, the quality and precision of surgery, specially at small scales, has been heightened through the use of robots and teleoperation surgeries (Howe and Matsuoka, 1999) (Bianchini et al., 2019).

The HMI in the areas of advanced training and rehabilitation have been the main motivation for the development of this work. Robotic machines provide an invaluable contribution to these areas by combining exercise physiology with technology (Jung et al., 2012) (De las Casas, 2017). Moreover, they have the capacity to produce workloads even in lack of gravity showing potential applications for instance in microgravity. The efficiency of the human training is highly important, specially in the space, where it plays a crucial role. Humans operating in lack of gravity for long time periods are exposed to the loss of muscle mass and bone density (Ploutz-Snyder et al., 2015). However, robotic machines promise to be beneficial to diminish these detrimental effects (A. Hargens and Friden, 1989) (Vogt and Hoppeler, 2014).

Real-time experiments have always played a key role in HMI developments (Ghaoui, 2005). However, a successful experiment is usually result of a good mathematical model and simulation. Consequently, in order to ensure a desirable performance, simulation tests should be carried out before any real-time experiments. Simulation tests have not been a problem in HMI on the side of the machine. Nonetheless, the lack of accurate human models suggests the existence of a gap. To achieve an accurate model simulation or to adapt a model previously developed can be challenge but highly important (Rahman and Mizukawa, 2013). HMI simulation models for English conversations between people and a humanoid robot have been reported (Khummongkol and Yokota, 2016). The simulation model was developed to help old people with comprehending problems. Another human model for people with abnormal hip stress distribution has been reported (Tsumura, 2008). Surgeries are extremely recommended to avoid worsening the disease. However, the optimal surgery procedure can be an arduous process. A simplified human model was the solution to deal with the problem and to support the preoperative planning. And alternatively, this novel method based on a feedback controller of the dynamics of a muscle-driven system is introduced to be used on human training and rehabilitation simulations with muscle activation estimations. This controller for muscle-driven system models makes possible to not only simulate the environment of interaction between a human and a robot, but also to make use of the state estimations as a feedback to regulate the robot behavior.

The presented method has been developed to control muscle-driven systems. It is based on the backstepping theory for position regulation. This work was originally built on a framework for a lower body muscle-driven (Richter and Warner, 2017). In order to validate the approach, a shoulder model composed by a group of eight

linkages, eight muscles and 3 degrees of freedom (DOFs) was used as an application example. The shoulder was conceived as a single ball and socket joint. Therefore, the three DOFs are allowed in a single point. The proposed method shows its ability to control the position and orientation of the shoulder muscle-driven system through muscular activation with redundancy resolution through least squares.

The remainder of the paper is organized as follows: Section 2 derives the dynamics of a general muscle-driven system including the linkage and muscle dynamics. Section 3 develops the feedback controller for any muscle driven-system. Section 4 provides the shoulder model dynamics used as the application example. Section 5 shows and discussed the results that validate the developed method. And finally, in Section 6 the conclusions are presented and the future work is stated.

2. MUSCLE DRIVEN DYNAMICS

The controller proposed in this work makes use of the mathematical model representation of the muscle driven system. This mathematical model is composed by two submodels. The first submodel represents the actuated linkage dynamics.

2.1 Actuated Linkage Dynamics

The linkage dynamics (M.W. Spong and Vidyasagar, 2005) given in joint coordinates are derived as:

$$D(q)\ddot{q} + C(q, \dot{q})\dot{q} + g(q) = \tau_m, \quad (1)$$

where q is a vector of joint displacements, $D(q)$ is the inertia matrix, $C(q, \dot{q})$ is the centripetal and Coriolis effects, $g(q)$ is the gravity vector, and τ_m is the control torque produced by the muscle torques.

2.2 Muscle Dynamics

The second submodel represents the muscle dynamics. The linkage dynamics 1 are controlled by the muscle torques τ_m . These torques are the product of the moment arm and the linear force of the muscle acting on the center of rotation of the joint (Sherman et al., 2013). The torques are computed as follows:

$$\tau_m = \vec{d}_m \times \vec{F}_m, \quad (2)$$

where d_m and F_m are the moment arm and the muscle force vectors. The muscle force vector is derived as:

$$\vec{F}_m = \vec{M}_u(\Phi), \quad (3)$$

where \vec{M}_u is the unit vector representing the orientation of the muscle, and Φ is the scalar value of the force along the muscle. The force on the muscle is calculated in function of the length of the serial element or the parallel/passive element according with the muscle representation of the Hill-type model (see Fig. 1).

Hill-type Muscle Model The Hill-type muscle model conceives the musculoskeletal system as a mechanical system (see Fig. 2). The hill-type muscle model relates the tension with the velocity (regarding the internal thermodynamics) (Kistemaker et al., 2013). The Hill-type muscle model (see Fig. 3) consists of following three elements:

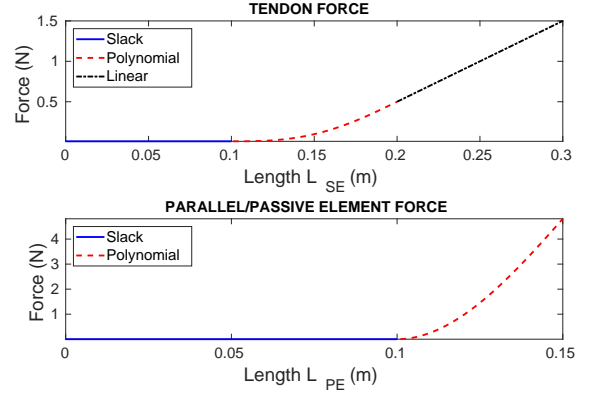


Fig. 1. Muscle force in function of the muscle elements length.

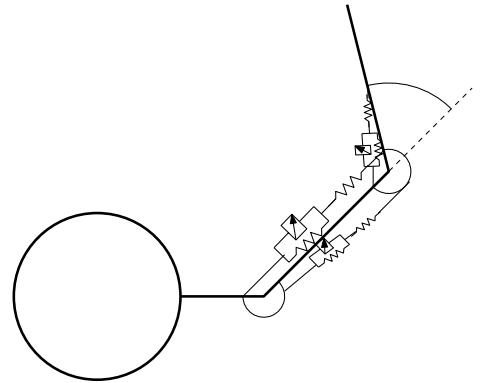


Fig. 2. Muscles represented as a mechanical system.

- A parallel elastic element (PE): Representing the collagen tissue.
- A contractile element (CE): Representing the contractile properties.
- A serial element (SE): Representing the tendinous tissue.

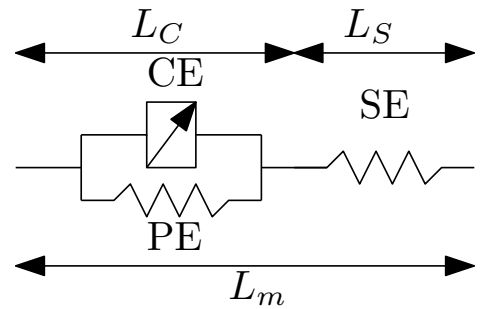


Fig. 3. Hill-type muscle model.

The length of the muscle L_m is computed as:

$$L_m = L_{CE} + L_{SE}, \quad (4)$$

where the L_{CE} and L_{SE} are the length of the contractile and serial element respectively. Besides, the rate of change of the contractile element length represents the activation on the muscle ($-\dot{L}_{CE} = u$). This activation u served as the control input to the muscle control. Consequently, from Eqn. 4, the speed of contraction for the serial element \dot{L}_{SE} is derived as:

$$\dot{L}_{SE} = \dot{L}_m + u \quad (5)$$

3. FEEDBACK CONTROLLER

The feedback controller proposed in this work is based on the backstepping theory (A. Raptis and Valavanis, 2011).

3.1 Feedback Control by Backstepping

From Eqn. 1, a synthetic control is defined as the control torque ($\zeta \triangleq \tau_m$). And a feedback law $\Psi(e)$ for tracking control is introduced. The variable e denotes the tracking error as

$$e = \begin{bmatrix} \tilde{q} \\ \dot{\tilde{q}} \end{bmatrix} = \begin{bmatrix} q - q_{des} \\ \dot{q} - \dot{q}_{des} \end{bmatrix} \quad (6)$$

The feedback law $\Psi(e)$ is built on the basis of inverse dynamics (Featherstone, 2008) as follows:

$$Da + C(q, \dot{q})\dot{q} + g(q), \quad (7)$$

where a is the synthetic acceleration defined as $a = \ddot{q}_{des} - Kd\dot{\tilde{q}} - Kp\tilde{q}$ with Kd and Kp as diagonal matrices of positive gains.

A control error w is defined as the difference between the synthetic control and the synthetic feedback law ($w = \zeta - \Psi$).

A perfect tracking ($e = [0, 0]^T$) and a decreasing positive definite Lyapunov function are assumed when the synthetic control and the synthetic feedback law are equal ($w = 0$).

When the control error is not zero ($w \neq 0$), the error dynamics can be found by rewriting the dynamic equation for the actuated linkage system (Eqn. 1) as

$$M(q)\ddot{q} + C(q, \dot{q})\dot{q} + g_v(q) = \zeta = \Psi + w, \quad (8)$$

and by substitution of the inverse dynamics from Eqn. 7, the control error is defined as:

$$w = M\ddot{\tilde{q}} + MK_d\dot{\tilde{q}} + MK_p\tilde{q} \quad (9)$$

Thereby, the error dynamics (e) are designated as

$$\dot{e} = Ae + Bw, \quad (10)$$

where

$$A = \begin{bmatrix} 0 & I \\ -K_p & -K_d \end{bmatrix} \quad \text{and} \quad B = \begin{bmatrix} 0 \\ M^{-1} \end{bmatrix}. \quad (11)$$

3.2 Lyapunov Function

The Lyapunov function is derived as

$$V = e^T P e + w^T R w, \quad (12)$$

where $P = P^T > 0$ and $R = R^T > 0$ to ensure the positive definiteness.

The time derivative of the Eqn 12 is computed using Eqn. 10 as follows

$$\dot{V} = -e^T Q e + 2w^T (B^T P e + R(\dot{\zeta} - \dot{\Psi})) \quad (13)$$

The negative-definiteness of \dot{V} (Eqn. 13) is enforced by making

$$2w^T (B^T P e + D(\dot{\zeta} - \dot{\Psi})) = -\Gamma w, \quad (14)$$

where $\Gamma = \Gamma^T > 0$. And by solving Eqn. 14 for the time derivative of the synthetic control $\dot{\zeta}$

$$\dot{\zeta} = \dot{\Psi} - R^{-1}(\Gamma w + B^T P e) \quad (15)$$

3.3 Control Input

From Eqn. 5, the control input (in matrix form) is represented as

$$U_i = \dot{L}_i - \dot{S}_i, \quad (16)$$

where S_i (the vector of series element lengths) is part of the derivative of the synthetic control ($\dot{\zeta}$)

$$\dot{\zeta} = \frac{\partial \tau_i}{\partial q_i} \dot{q}_i + \left[\frac{\partial \tau_i}{\partial S_i} \right]^T \dot{S}_i \quad (17)$$

Using the value calculated for $\dot{\zeta}$ in Eqn. 15 and replacing Eqn. 16 in Eqn. 17, the control input is calculated as

$$U_i = \left(\left[\frac{\partial \tau_i}{\partial S_i} \right]^T \right)^+ \left(\dot{\zeta}_i - \frac{\partial \tau_i}{\partial q_i} \dot{q}_i - \left[\frac{\partial \tau_i}{\partial S_i} \right]^T \dot{L}_i \right) \quad (18)$$

Where N^+ represents the pseudoinverse of N .

4. APPLICATION EXAMPLE

The approach is validated by using a shoulder musculoskeletal system. The system was modeled as a group of eight linkages, eight muscles and 3 DOFs (see Fig. 4). The model dynamics are available for free download at (De las Casas, 2019).

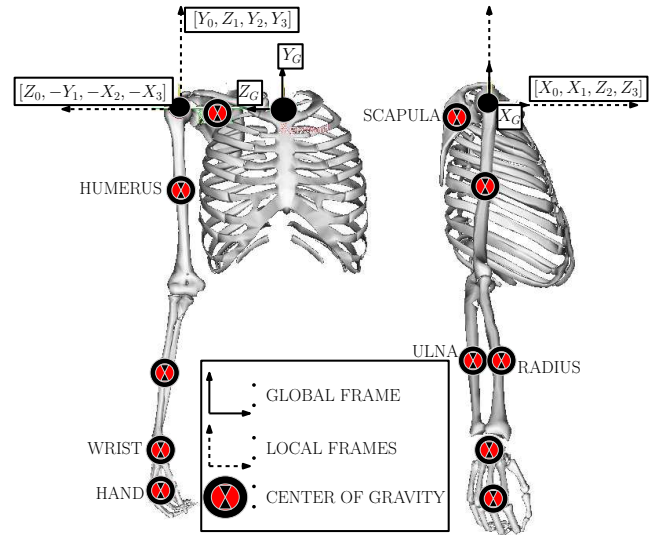


Fig. 4. Upper arm skeletal system and frames.

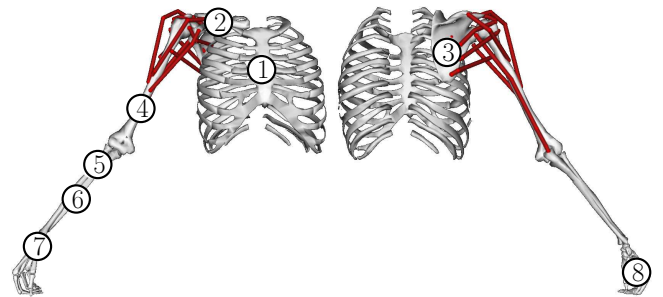


Fig. 5. Simulated bodies (anterior and posterior musculoskeletal system view).

The shoulder model (including muscles and bones length, mass, inertia and center of mass) was developed based on the real parameters of a person with 1.8 meters of tall

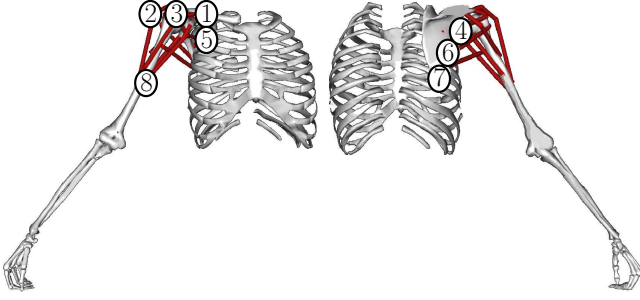


Fig. 6. Simulated muscles (anterior and posterior musculoskeletal system view).

Table 1. Linkages of the musculoskeletal system.

N ^o	Linkage	Position (relative to)	Attached Muscles
1	Ground	Fixed	0
2	Clavicle	Fixed (Ground)	1
3	Scapula	Fixed (Clavicle)	9
4	Humerus	Mobile (Scapula)	9
5	Ulna	Fixed (Humerus)	1
6	Radius	Fixed (Ulna)	0
7	Wrist	Fixed (Radius)	0
8	Hand	Fixed (Wrist)	0

and a mass of 75.16 kg. The data was extracted using the OPENSIM software (Delp et al., 2007). The OPENSIM model used was originally developed for the complete upper body (Saul et al., 2015).

A total of eight linkages and eight muscles were selected to fit the model (see Fig. 5 and Fig. 6). Three of the eight linkages are fixed to ground (see Table. 1). The selection of the muscles has been done based on those which have contribution to the shoulder movement. Due to the large size of the deltoid, the muscle was modeled as two individual smaller muscles (Deltoid-1 and Deltoid-2). The muscle architecture is listed on Table. 2.

Table 2. Muscles in the musculoskeletal system.

N ^o	Muscle	Attachment-1	Attachment-2
1	Deltoid-1	Humerus	Clavicle
2	Deltoid-2	Humerus	Scapula
3	Supraspinatus	Humerus	Scapula
4	Infraspinatus	Humerus	Scapula
5	Subscapularis	Humerus	Scapula
6	Teres Minor	Humerus	Scapula
7	Teres Major	Humerus	Scapula
8	Coracobrachialis	Scapula	Humerus

The musculoskeletal system aims to mimic the movement of the shoulder. It was conceived as a single ball and socket joint. Hence, the three DOFs are allowed in a single point and are controlled by the eight selected muscles. The dynamic model of the system was developed following the DH convention (see Table 3) and its dynamics in joint coordinates are represented by the previous Eqn. 1, where $q^T = [q_1, q_2, q_3]$ is a vector of joint displacements, q_1 is the flexion displacement, q_2 is the inward rotation displacement and q_3 is the adduction displacement, $D(q)$ is the inertia matrix of the arm, $C(q, \dot{q})$ accounts for the centripetal and Coriolis effects, $g(q)$ is the gravity vector and $\tau_{muscles}$ are the torques generated by the muscle forces.

Table 3. Frames of the musculoskeletal system.

Frame	Translation	DH			
		θ	d	a	α
Global	0	0	0	0	0
0	Humerus _(x;y;z)	0	0	0	0
1	0	q1	0	0	$-\frac{\pi}{2}$
2	0	q2	0	0	0
-	0	$\frac{\pi}{2}$	0	0	$\frac{\pi}{2}$
3	0	q3	0	0	0

Table 4. Desired position, velocity and acceleration per DOF.

DOF	Target Position (DEG)	Initial Position (DEG)
1	50°	$50^\circ \pm 10^\circ$
2	27°	$27^\circ \pm 10^\circ$
3	-45°	$-45^\circ \pm 10^\circ$

The simulations are performed in order to move the arm to a static holding-a-cup position. The initial joint positions are randomly selected between $\pm 10^\circ$ from the desired final positions (see Table. 4).

5. RESULTS AND DISCUSSION

The Lyapunov function and its time derivative can be seen on Fig. 7. Based on the positive definition of the Lyapunov function, the negative semi-definition of its time derivative and an expected convergence for both, the stability of the system is proved. Furthermore, from Fig. 8 can be seen that the states converge to the desired values in approximately 3.5 seconds. Consequently, the target position is successfully achieved by solving the muscle redundancy resolution.

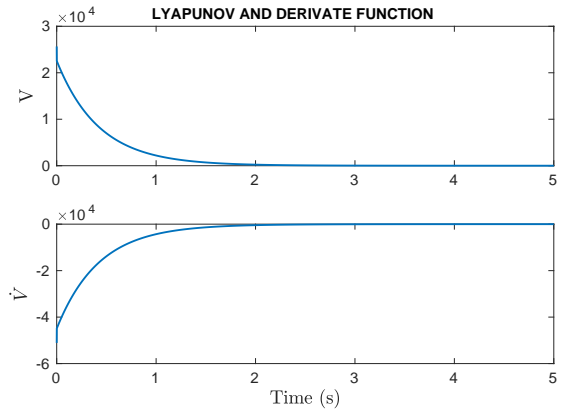


Fig. 7. Lyapunov and its derivative function.

The required muscle activations obtained to achieved the desired trajectory are shown in the following figures (Fig. 9, 10, 11 and 12). Results show a convergence in each of the muscles. These converged values seem to be related to the required activations to overcome the gravity in the final position. The muscle activations show realistic values of magnitude and shape. However, it is difficult to quantify it without real-time experiments under the same experimental conditions. The muscles supraspinatus, infraspinatus, teres minor and coracobrachialis have shown the highest activation values. These highest activation makes sense due to the target position to be reached out.

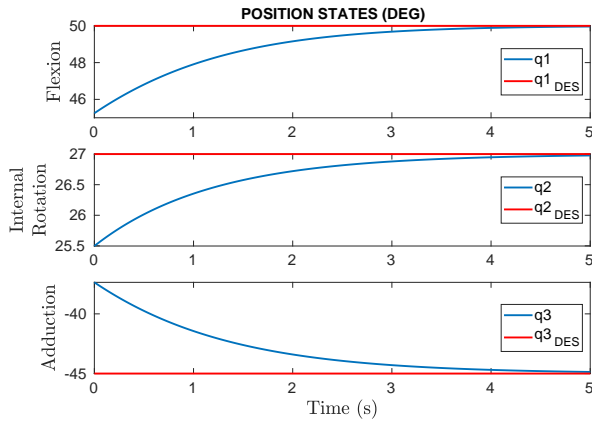


Fig. 8. Position tracking.

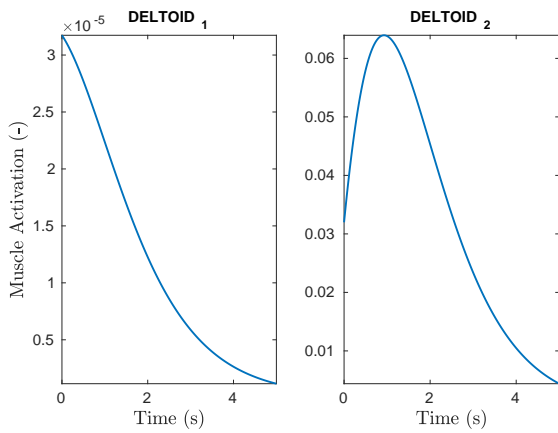


Fig. 9. Muscle activation of the Deltoid-1 and Deltoid-2.

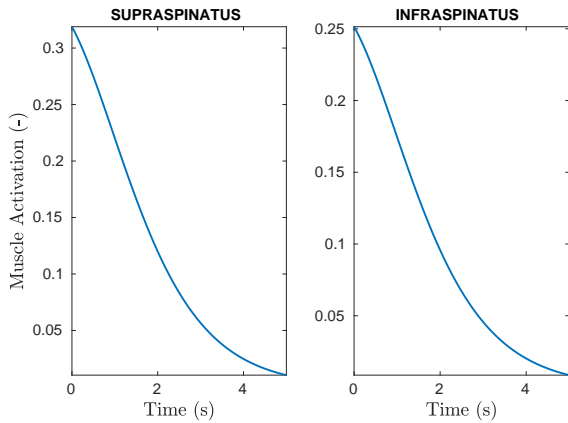


Fig. 10. Muscle activation of the Supraspinatus and Infraspinatus.

6. CONCLUSION AND FUTURE WORK

Upon completion of the feedback controller simulations on the shoulder model, realistic muscle activations were witnessed. Thus, the effectiveness of the feedback controller to solve muscle driven system with redundancy resolution is shown. It is important to consider that variations in the musculoskeletal distribution of the model, as well as a different dynamic models, can vary the results.

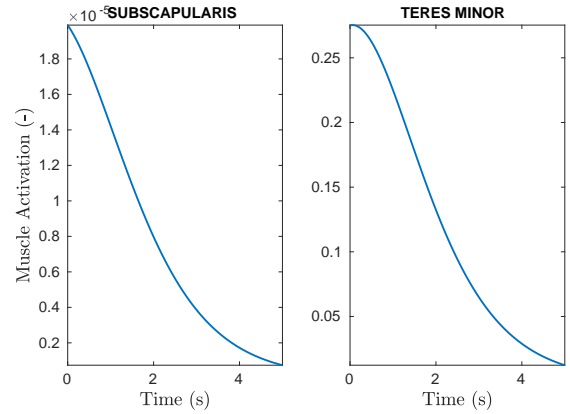


Fig. 11. Muscle activation of the Subscapularis and Teres Minor.

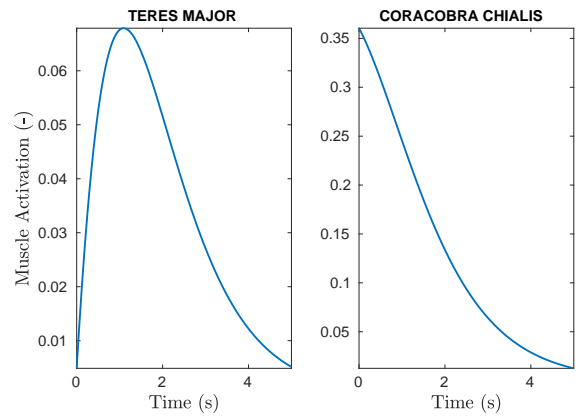


Fig. 12. Muscle activation of the Teres Major and Coracobra Chialis.

The feedback controller was successfully tested in simulation with the shoulder model. The objective of moving the arm from a static position to another one was achieved showing realistic results. Furthermore, results show a convergence on the muscle activations. This convergence suggests that the controller is effective finding the required muscle activation values to overcome the gravity effect on the musculoskeletal weight in the final position. Future research will be performed to compare these simulation results with real-time experiments with the same objectives.

Several applications can make use of this method. Beyond the control tracking developed, the method can be adapted for different objectives. Some possible adaptations can be oriented to the optimization of human training or rehabilitation practices. For instance, advanced exercise machines could make use of the muscle activation as a feedback for performance improvement (through targeting or maximization of muscle activation). Likewise, rehabilitation developments could make use of the estimated muscle activation in order to provide a better assistance. Based on the muscle activation feedback, maximization of some muscle activation with minimization of others can be achieved.

In future developments, besides of more complex trajectories, more realistic and complete models will be used for testing the current approach. Further research will

also include the integration of multiple control systems for human machine interaction related to advanced exercise machines and rehabilitation.

ACKNOWLEDGEMENTS

This research was supported by the NSF, grant 1544702.

REFERENCES

- A. Hargens, S. Parazynski, M.A. and Friden, J. (1989). Muscle changes with eccentric exercise: Implications on earth and in space. Technical report, NASA.
- A. Raptis, I. and Valavanis, K. (2011). Linear and nonlinear control of small-scale unmanned helicopters. 45. doi:10.1007/978-94-007-0023-9.
- Bianchini, M., Palmeri, M., Stefanini, G., Furbetta, N., and Di Franco, G. (2019). The role of robotic-assisted surgery for the treatment of diverticular disease. *Journal of Robotic Surgery*. doi:10.1007/s11701-019-01008-y. URL <https://doi.org/10.1007/s11701-019-01008-y>.
- Chang, W.H. and Kim, Y.H. (2013). Robot-assisted therapy in stroke rehabilitation. *Journal of Stroke*, 15, 174–181.
- De las Casas, H., Richter, H., and van den Bogert, A. (2017). Design and hybrid impedance control of a powered rowing machine. In *ASME 2017 Dynamic Systems and Control Conference*.
- De las Casas, H. (2017). *Design and Control of a Powered Rowing Machine with Programmable Impedance*. Master's thesis, Cleveland State University.
- De las Casas, H. (2019). Shoulder-model-3d-v1. <https://github.com/HumbertoDlc/Shoulder-Model-3D-V1>.
- De las Casas, H., Kleis, K., Richter, H., Sparks, K., and Antonievan den Bogert (2019). Eccentric training with a powered rowing machine. *Medicine in Novel Technology and Devices*, 2, 100008.
- Delp, S., Anderson, F., Arnold, A., Loan, P., Habib, A., John, C., Guendelman, E., and Thelen, D. (2007). Opensim: Open-source software to create and analyze dynamic simulations of movement. *Biomedical Engineering, IEEE Transactions on*, 54, 1940 – 1950. doi: 10.1109/TBME.2007.901024.
- Featherstone, R. (2008). *Inverse Dynamics*, 89–100. Springer US, Boston, MA. doi:10.1007/978-1-4899-7560-7_5. URL https://doi.org/10.1007/978-1-4899-7560-7_5.
- Ghaoui, C. (2005). *Encyclopedia of Human Computer Interaction*. Information Science Reference - Imprint of: IGI Publishing, Hershey, PA.
- Howe, R.D. and Matsuoka, Y. (1999). Robotics for surgery. *Annual Review of Biomedical Engineering*, 1(1), 211–240. doi:10.1146/annurev.bioeng.1.1.211. PMID: 11701488.
- Jung, D.W., Park, D.S., Lee, B.S., and Kim, M. (2012). Development of a motor driven rowing machine with automatic functional electrical stimulation controller for individuals with paraplegia: a preliminary study. In *Annals of Rehabilitation Medicine*, 379–385.
- Khalaf, P., Richter, H., Van Den Bogert, A., and Simon, D. (2015). Multi-objective optimization of impedance parameters in a prosthesis test robot. In *ASME 2015 Dynamic Systems and Control Conference*, volume 3.
- Khalaf, P., Warner, H., Hardin, E., Richter, H., and Simon, D. (2018). Development and experimental validation of an energy regenerative prosthetic knee controller and prototype. In *ASME 2018 Dynamic Systems and Control Conference*, volume 1.
- Khummongkol, R. and Yokota, M. (2016). Computer simulation of human-robot interaction through natural language. *Artificial Life and Robotics*, 21(4), 510–519.
- Kistemaker, D., Van Soest, A., Wong, J., Kurtzer, I., and Gribble, P. (2013). Control of position and movement is simplified by combined muscle spindle and golgi tendon organ feedback. In *Journal of Neurophysiology*.
- M.W. Spong, S.H. and Vidyasagar, M. (2005). *Robot Modeling and Control*. Wiley.
- Ploutz-Snyder, L., Ryder, J., English, K., Haddad, F., and Baldwin, K. (2015). Risk of impaired performance due to reduced muscle mass, strength, and endurance. Technical report, NASA.
- Rahman, M.A.A. and Mizukawa, M. (2013). Model-based development and simulation for robotic systems with sysml, simulink and simscape profiles. *International Journal of Advanced Robotic Systems*, 10(2), 112. doi: 10.5772/55533.
- Richter, H. and Warner, H. (2017). Backstepping control of a muscle-driven linkage. In *2017 IFAC World Congress*.
- Saul, K.R., Hu, X., Goehler, C.M., Vidt, M.E., Daly, M., Velisar, A., and Murray, W.M. (2015). Benchmarking of dynamic simulation predictions in two software platforms using an upper limb musculoskeletal model. In *Computer Methods in Biomechanics and Biomedical Engineering*.
- Schmidt, H., Werner, C., Bernhardt, R., Hesse, S., and Krger, J. (2007). Gait rehabilitation machines based on programmable footplates. *Journal of NeuroEngineering and Rehabilitation*.
- Sherman, M., Seth, A., and Delp, S. (2013). What is a moment arm? calculating muscle effectiveness in biomechanical models using generalized coordinates. volume 2013. doi:10.1115/DETC2013-13633.
- Tsumura, H. (2008). A computer simulation in surgery for a human hip joint. *Artificial Life and Robotics*, 12(1), 14–17.
- Vogt, M. and Hoppeler, H.H. (2014). Eccentric exercise: mechanism and effects when used as training regime or training adjunct. In *The American Physiological Society*, 116, 1446–1454.